PNM Field Experience—Single-Pole Trip and Reclose Near High IBR Generation

Daniel Marquis, Errol Singer, Melvin Bowekaty, and Chelsea Collette
Public Service Company of New Mexico

Samir Dahal
Siemens Gamesa

Ashish Parikh, Milind Malichkar, and Kamal Garg
Schweitzer Engineering Laboratories, Inc.

Presented at the
79th Annual Georgia Tech Protective Relaying Conference
Atlanta, Georgia
April 15–17, 2026

Previously presented at the
79th Annual Conference for Protective Relay Engineers, March 2026

Previously revised editions released October 2025 and November 2025

Originally presented at the
52nd Annual Western Protective Relay Conference, October 2025

PNM Field Experience—Single-Pole Trip and Reclose Near High IBR Generation

Daniel Marquis, Errol Singer, Melvin Bowekaty, and Chelsea Collette, *Public Service Company of New Mexico*
Samir Dahal, *Siemens Gamesa*
Ashish Parikh, Milind Malichkar, and Kamal Garg, *Schweitzer Engineering Laboratories, Inc.*

***Abstract*—Public Service Company of New Mexico, an energy utility, has committed to achieving zero emissions by 2040, which has prompted the growth of renewable energy resources in their electric grid, thus increasing the penetration of inverter-based resources (IBRs) into the system. IBRs provide additional load support and improve the renewable energy portfolio of the utility; however, IBRs also pose many challenges to the existing extra-high voltage (EHV) transmission line protection system of the utility. With the goal of modernizing their line protection technology to overcome these challenges and obtain system-wide consistency, the utility standardized their EHV transmission line protection to include ultra-high-speed line relays, which is described in the paper "Protecting EHV Transmission Lines Using Ultra-High-Speed Line Relays: A New Standard for PNM," presented at the Western Protective Relay Conference in 2021.**

This paper details the utility's single-phase tripping (SPT) and reclosing philosophy on 345 kV lines, many of which are connected to large renewable generation. Based on field experience, these philosophies evolved to meet the ride-through requirements during single-pole trip and reclose operations. The utility standard suggests using a neutral reactor (fourth-leg reactor) for secondary arc extinction. This paper provides field events showing the response of the differential and pilot schemes, and noncommunications-based protection elements for faults on the 345 kV lines connected to renewable generation. The utility has both Type 3 and Type 4 renewable generation, and the fault current contributions are quite different compared to conventional generation.

I. Introduction

Public Service Company of New Mexico (PNM) is the largest energy provider in New Mexico, operating over 3,000 miles of transmission line network, a significant portion of which is also used by other utilities and independent producers to supply power in New Mexico, Arizona, and California. The utility plans to achieve zero emissions by 2040 and uses a diverse mix of generation resources including hundreds of megawatts of wind, solar, and battery energy resources, which are being integrated into the electric grid in conjunction with user-owned renewables programs. Fig. 1 shows a section of the utility's system that uses a single-pole tripping (SPT) and reclosing scheme. It is a relatively isolated 345 kV portion of the system, which includes over 2 GW of a mix of Type 3 and Type 4 wind generation, a series capacitor, shunt reactors with neutral grounding reactors (NGRs), a synchronous condenser, and a static VAR compensator (SVC) (see Fig. 1). In Fig. 1, the letters inside the boxes represent substations within the utility's system. The typical direction of the load flow is from the wind farms and the high-voltage direct current (HVdc) converter on the right side of the figure toward the utility's system on the left. Of note, there is no load in the area, so the system is overbuilt to 362 kV nominal voltage standards. Protection consists of communications-assisted permissive overreaching transfer trip (POTT) and differential schemes, along with step-distance and ground time-overcurrent backup elements.

Disruptions to the system in Fig. 1 can result in long restoration times and equipment restart challenges. Therefore, SPT and reclosing schemes are used in this area to improve system availability. The use of SPT schemes started early on when the system was simply a long 345 kV line to a 200 MVA HVdc converter and has continued up until today. Presently, the system has more than 2 GW of interconnected energy resources, multiple stations, and additional lines and devices. Several wind farms aim to ride through SPT, and this paper examines theory, practical challenges, and real-world implementation of SPT events.

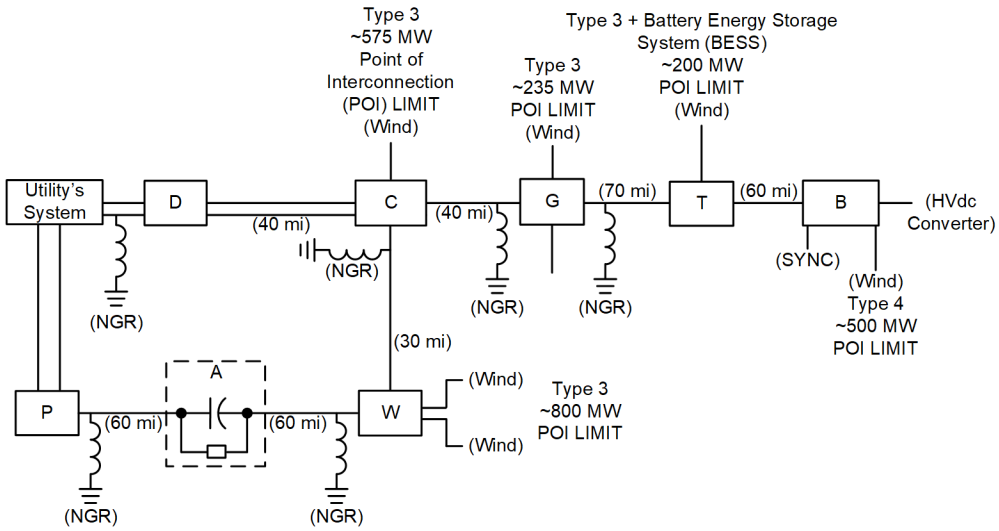

Fig. 1. Simplified One-Line Diagram of the Utility's System–345kV Nominal Voltage Section With SPT and Reclosing Schemes

II. SPT Protection Practice and Philosophy

The utility applies SPT schemes in select portions of its extra-high voltage (EHV) transmission system. SPT schemes are particularly beneficial in systems with high renewable energy penetration and long transmission lines, where maintaining system stability and minimizing fault-related disruptions are critical. In transmission lines equipped with SPT and reclosing schemes, only the faulted phase is disconnected during a single-phase-to-ground fault, while the remaining two phases continue to operate. This approach helps preserve power flow and reduces the impact on connected generation resources. However, during the single-phase open interval, the disconnected phase is subject to induced voltage caused by capacitive and inductive coupling from the two energized phases. This induced voltage can sustain a secondary arc at the fault location, which may interfere with successful reclosing and delay fault clearance.

The utility provides four-legged reactors (with a neutral inductance) to EHV and high-voltage lines where SPT is used. The neutral reactor helps extinguish the secondary arc maintained by the capacitive coupling from the remaining two healthy phases. Fig. 2 shows an example of the overall protection scheme and the utility's practice for a series-compensated line with a line reactor and SPT [1] [2] [3]. The one-line diagram in Fig. 2 shows the scheme with breaker-and-a-half arrangement and three relays for protection. Main 1 and Main 2 are line current differential relays with distance and reclosing. Main 3 is an ultra-high-speed (UHS) relay with no reclosing. All the relays trip independently.

The utility employs SPT on select 345 kV lines, as shown in Fig. 1, to ensure continuity of the energy transmission service. The utility uses three relays at this voltage level; two relays are phasor-based line differential relays and the third relay is a UHS line relay with POTT. Fig. 2 shows a typical protection scheme.

The utility's methodology is to single-pole trip and automatically reclose only one breaker per line end. The second breaker is three-pole tripped and is later manually reclosed via supervisory control and data acquisition (SCADA) by operations. The utility uses four-legged reactors with a neutral inductance to help with secondary arc deionization and thereby helps ensure the successful reclosing of the open phase. Synchronous condensers and SVCs are connected to the transmission systems, providing voltage and inertia system support. The utility has successfully applied a dead time of approximately 25 to 30 cycles, along with a ride-through capability for SPT near a high inverter-based resource (IBR) penetration area. This approach is further discussed in Sections IV and V.

The two phasor-based protection relays have identical functionality and settings criteria. Both systems operate in parallel to initiate tripping and, when appropriate, single-pole automatic reclosing. In contrast, the UHS relay uses time-domain technology alongside phasor-based elements and schemes, including SPT, for high-speed tripping. It is used to provide protection diversity but does not independently initiate automatic reclosing.

For the two phasor-based relays, high-speed trip and single shot reclose are initiated for communications-assisted phasor current ground differential or phasor POTT ground trips. In areas susceptible to stable power swings, phasor-based POTT trips are only allowed to trip if the redundant channel phasor current differential is partially or fully out of service. The utility's general philosophy is to use Z1 phase, Z1 ground, and overcurrent elements for tripping only when differential protection is out of service. POTT schemes with weak-infeed logic are also enabled as needed. At Station A, in Fig. 1, the utility allows single-phase bypass for series capacitor protection. In the event of a single-phase fault, only the faulted phase is triggered to bypass.

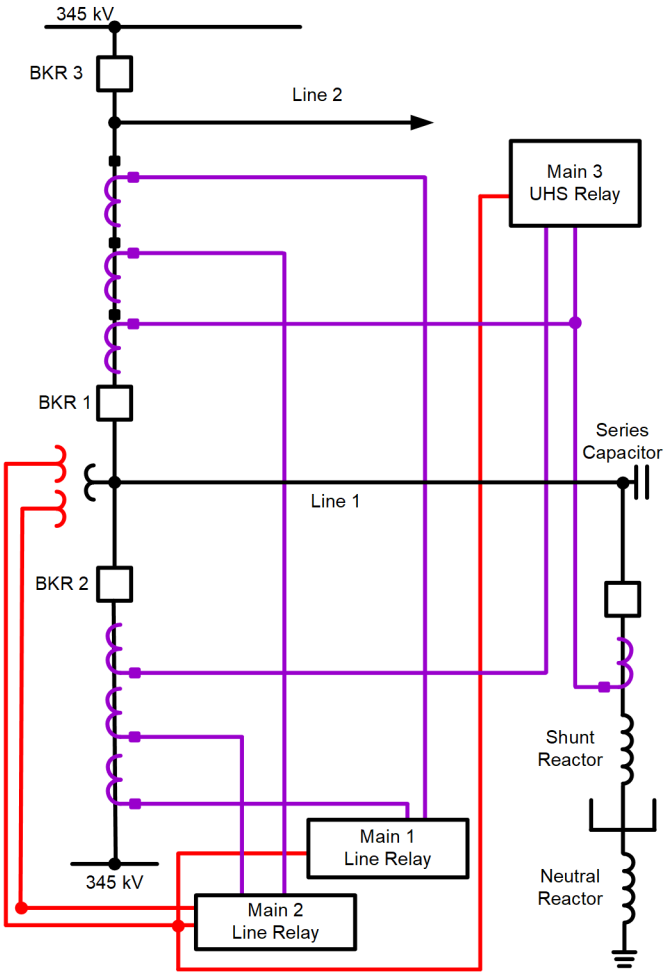

Fig. 2. Example Line Protection With SPT for Series-Compensated Lines

III. Introduction of SPT and IBR

The utility uses SPT in the corridor with IBR generation, as shown in Fig. 1. During SPT events, the system is still synchronized and connected via the two heathy phases. Type 3 and Type 4 inverters and fault contribution are discussed in various sources [1] [2] [3] [4] [5]. This section explains that IBRs do not provide a zero-sequence source; instead, the zero-sequence source is provided through the transformer connection path. Also, negative sequence is not being provided by Type 4 IBRs. Type 3 provides a negative sequence based upon the control system design. Later sections of this paper discuss the basics of directionality for forward and reverse faults. For additional reading and correct application of directional elements near IBRs, refer to Section IV and [4], [5], and [6].

A. Forward and Reverse Determination of Directional Elements for Traditional Sources

Fig. 3 and Fig. 4 illustrate a simple model of two conventional sources. The directional element is looking into Line 1. For a fault in the forward direction, with respect to the directional relay, the voltages and currents align, as shown in Fig. 3, for a totally inductive system with 90 degree angular differences between currents and voltages. For a fault in the reverse direction, the voltages and currents align, as shown in Fig. 4 and [4].

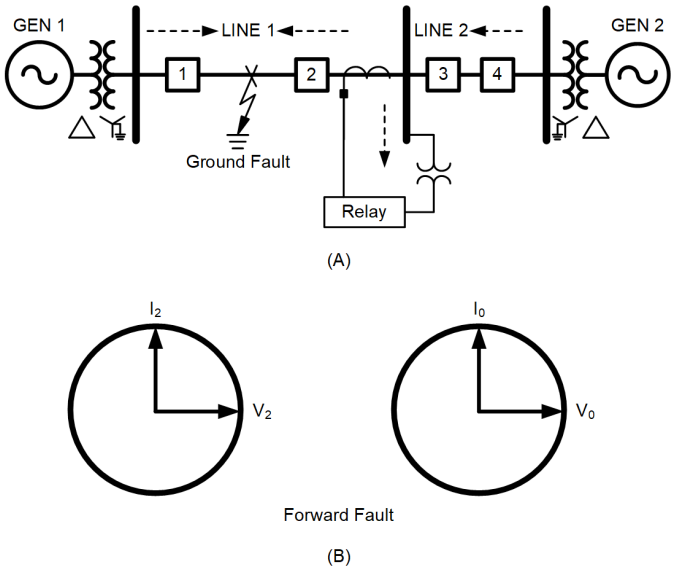

Fig. 3. Fault in the Forward Direction for the Directional Element

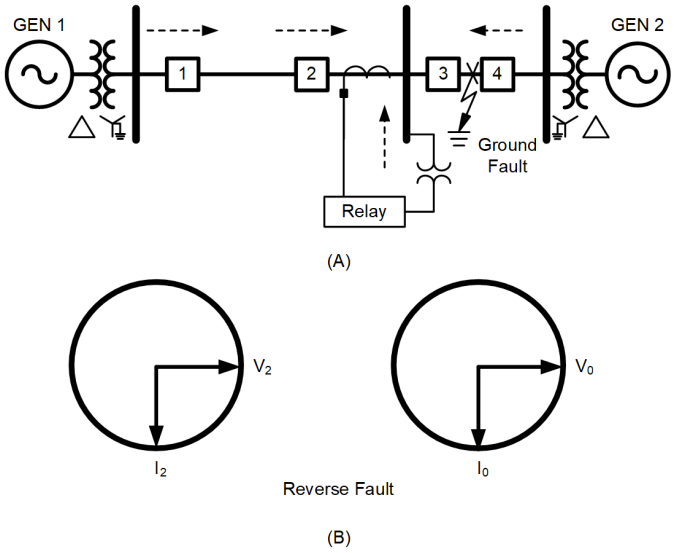

Fig. 4. Fault in the Reverse Direction for the Directional Element

B. Forward and Reverse Elements and Fault Currents With IBR Sources

It has been observed from various field events and sources that I2 relationships with respect to V2 voltage are not deterministic for the IBR sites [4] [5] [6]. The following field event indicates the operation of a Type 4 IBR site. Fig. 5 shows the 32.5-mile line with conventional generation at one end and wind generation (Type 4) at the other end. The responses of conventional versus renewable IBR generation are completely different for the same fault. Fig. 6 shows the response and signature of the fault response from conventional generation and IBR generation.

During the BG fault, currents increase at the IBR end, as well as in unfaulted phases, which is not at the conventional generation end. Additionally, it is observed that the I2 magnitude and angle substantially changes from the IBR end.

Substantial variations in magnitude and angle can lead to wrong directional decisions by the relay. As shown in Fig. 6, the IBR end negative-sequence current angle varies at time T1 and T2. As a result, when a relay uses I2, the direction cannot be determined reliably. As many other studies indicate, zero-sequence sources are more secure than negative-sequence sources. In IBR installations with the IBR transformer grounding, as shown in Fig. 5, zero sequence-based directional quantities are more reliable than those of negative sequence.

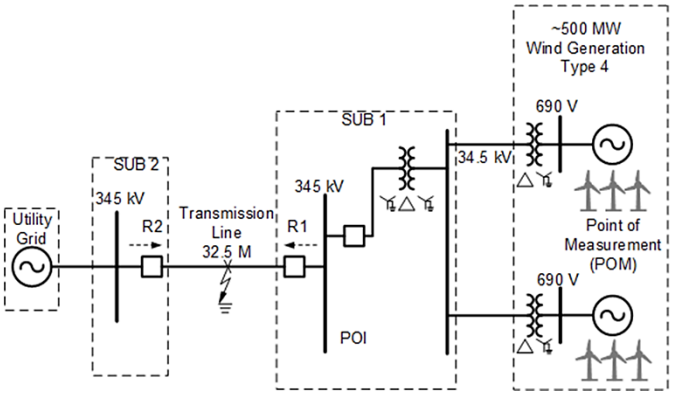

Fig. 5. Example of Conventional and IBR Interconnection With a Fault in the Transmission Line

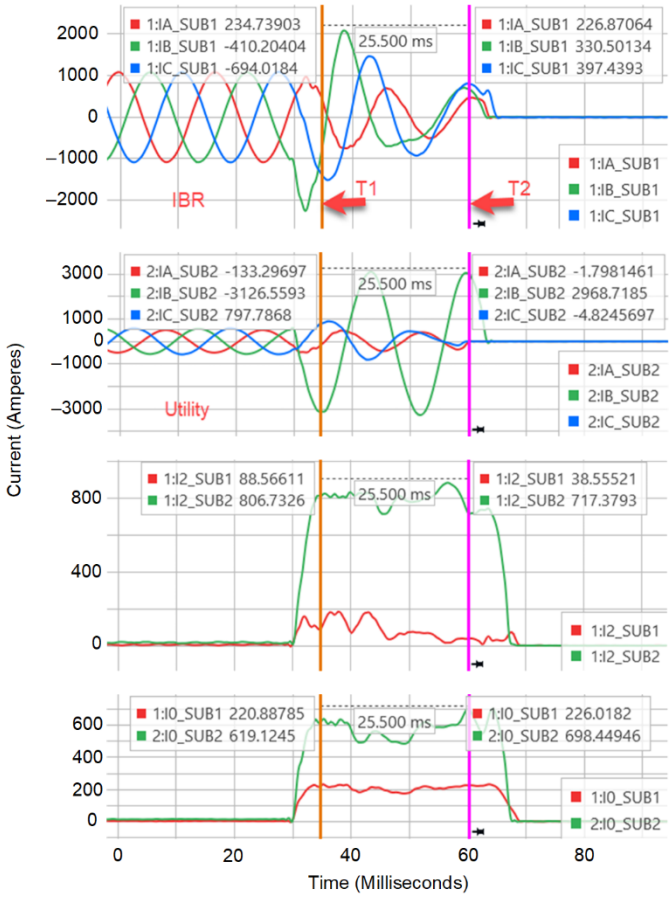

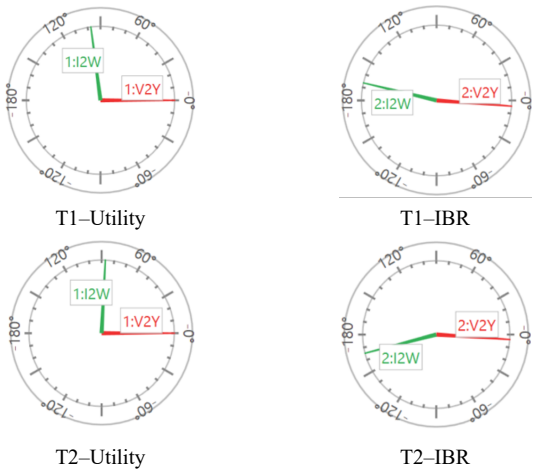

Fig. 6. Current Fault Contributions of Conventional (SUB 2) and IBR Sources (SUB 1) for a BG Internal Fault

IV. Known Challenges of SPT Near IBRs

Operating SPT schemes on transmission lines connected to IBRs presents several practical challenges. These include both protection system limitations and control-related issues unique to IBRs.

A. SPT Near IBRs and Challenges

Reduced fault current levels [6]: IBRs typically contribute fault current only slightly above their rated output due to current-limiting controls. This low fault current is often insufficient to satisfy the fault-overcurrent supervision thresholds of distance protection elements, preventing them from operating as intended and reducing their effectiveness in detecting and clearing faults.

Unbalanced fault response [6] [7]: SPT due to a line-to-ground fault introduces unbalanced voltage conditions that can challenge nearby IBRs. Type 4 IBRs, which are full converter systems, typically inject only positive-sequence current and do not actively respond to negative-sequence components. The resulting negative-sequence voltage can disrupt the phase-locked loop (PLL), which is critical for grid synchronization. Conventional PLLs may experience phase tracking errors or instability under such conditions, leading to degraded current control or delayed recovery. These effects are more pronounced when the fault occurs electrically close to the IBR. IEEE Std 2800-2022, *IEEE Standard for Interconnection and Interoperability of Inverter-Based Resources (IBRs) Interconnecting with Associated Transmission Electric Power Systems*, outlines performance expectations for IBRs [8].

Protection coordination challenges [9]: IBRs contribute low and variable fault currents, which can impair traditional protection schemes like POTT and directional comparison blocking. Line current differential protection (87L) is preferred as the primary scheme due to its sensitivity and independence from fault current magnitude or direction. POTT schemes with weak-infeed logic remain useful, enabling tripping even when fault current is minimal at one terminal. Distance elements are typically retained as backup or supervisory functions.

Voltage support limitations [6]: Without synchronous machines or condensers online, the system may lack adequate dynamic voltage support during SPT conditions. This can lead to deeper voltage dips on the unfaulted phases and slower voltage recovery after reclosing.

Breaker and reclosing concerns [10]: IBRs are sensitive to reclosing transients. If the breaker fails to reclose properly, or if a three-pole trip occurs instead of a single-pole trip, it can cause unnecessary inverter trips or power quality issues. Breaker health and timing are critical in these scenarios.

Ride-through and control stability [8]: During SPT events, IBRs must stay online and ride through the disturbance. However, if the voltage unbalance is too severe or lasts too long, the inverter may trip or lose synchronization. Ensuring proper low-voltage ride-through performance under these conditions is essential.

Grid-following (GFL) inverter limitations [7]: During three-pole tripping, GFL inverters relying on PLLs cannot operate independently without a reference grid. If the system is islanded or lacks a strong voltage source, GFL inverters may trip or fail to maintain synchronization, highlighting the need for grid-forming capabilities in critical areas.

B. Designing an SPT Scheme Near IBRs

When SPT and reclosing are desirable on the lines connecting renewable generation, certain aspects are important to consider. Some applications allow more than one line to connect, like a grid, to the renewable generation. However, for some applications, renewable generation may be connected via a radial line to the transmission substation or can be tapped off the transmission line. Based on one equipment manufacturer experience in the utility's grid, it was observed that Type 4 wind turbine generators (WTGs) (based on a full converter) were more prone to trip during SPT events due to their lack of natural response in providing negative-sequence current to alleviate the unbalance seen in the WTG terminals than Type 3 WTGs (doubly fed induction generators).

An example system was used for a lab test to validate the performance of IBRs during the SPT events. Fig. 5 shows the test system that was used. The lab test was done for a Type 4 wind farm WTG, and the fault was simulated at 25 miles from Substation 1 for a B-phase-to-ground fault. The measurement point was at the 690 V transformer for the windfarm controls.

Some of the challenges observed were renewable generation must be capable of riding through a one-phase open condition during reclosure dead time, which is typically 0.5 seconds but can vary from 0.5 to 1.0 seconds. Not every IBR renewable generator is capable of riding through such a condition and ability may vary depending on the exact nature of the system and reclosing behavior, so advance consultation with a renewable generation manufacturer is required.

Concern and difficulty arise with reactive power contribution from renewable generation during and immediately after an open-pole condition, particularly when the control is based on local measurements. In such cases, generation behavior may lead to excessive system voltage rise, posing operational challenges and potential risk of generator tripping.

For IBR sources, when the system is operating with only two phases in service on the transmission line, injecting power into the transmission system has been observed to increase the voltage on the healthy phases. One solution is to reduce the active power generation during the SPT event. The drawback of this solution is that a proper system needs to detect the SPT situation at the WTG terminals, where the voltage is measured.

For this application, Type 4 WTGs require specialized control to detect SPT events when a single-phase fault is cleared by the breakers. The control keeps the WTGs in voltage ride-through (VRT) mode, maintaining connection during the abnormal system voltage, while reducing active current until the faulted phase is cleared and the breaker is reclosed. However, Type 3 WTGs ride through the event without changes. This means keeping or driving the converter in the local control mode, which is the same behavior as during a ride-through mode, until the normal operation resumes.

IEEE 2800-2022, defines the ride-through requirements to avoid tripping during switching and transient events as1.2 pu voltage for 1.0 seconds [8]. Fig. 7 also defines the limit of transient overvoltage as 1.8 pu for 0.2 ms. Lab tests were done to meet these requirements, which are discussed in next section.

The turbine's protection logic is based on the root-mean-square (rms) voltage, which is measured at its terminals, rather than the specific type of fault occurring in the system. Whether the disturbance is a single-phase or a three-phase event, if the resulting terminal rms voltage drops or exceeds a predetermined threshold, the turbine will enter VRT mode and respond according to the grid ride-through requirements.

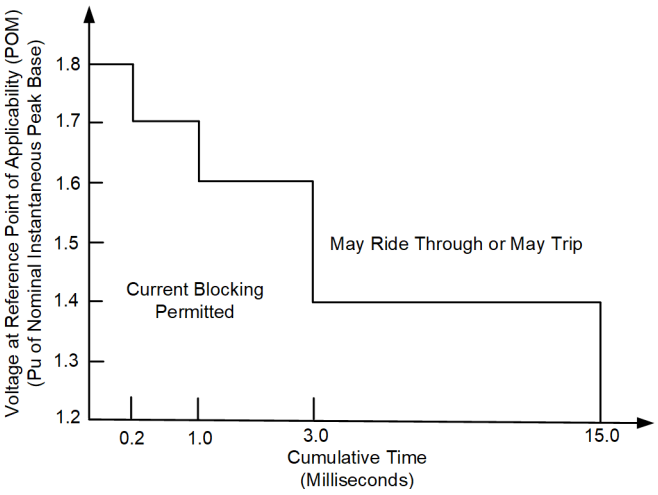

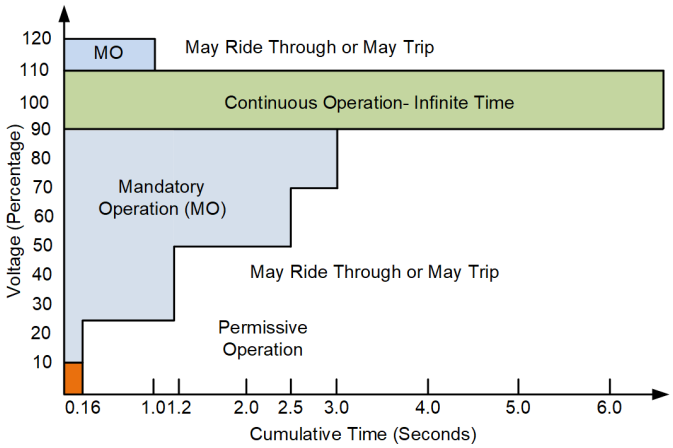

Fig. 7. Transient Voltage Ride Through for IBR Plant (IEEE 2800 [8] Figure: 11 and Figure D.6)

C. *Lab Test Results to Validate the SPT Near IBRs*

Unlike the application of the SPT in conventional systems where off-the-shelf protective relays can be used, the presence of renewable generation on the protected line requires consultations with a renewable generation manufacturer and grid operator, possibly involving detailed simulations prior to commencing with a design. Simulation testing is required to test and demonstrate that WTG controls can ride through SPT events in the specific transmission network and during various SPT events.

For most applications, WTGs' protection systems are configured on rms values. WTGs' controls do not react to the instantaneous values alone. WTGs' reactions are dictated by the voltage on their terminal (690 V side), since that is the conventional measurement point used by the converters to avoid communication delays for any other upwards measurement. For Type 4 WTGs, the lack of natural negative-sequence current injection results in significant overvoltage at the generator terminals. This overvoltage results in extremely high dc voltage tripping the turbine. However, Type 3 WTGs are able to aid in balancing the voltages at the terminal through negative-sequence current injections and thus prevent the overvoltages when the fault is cleared.

Fig. 8 illustrates 18-cycles fault on the B-phase that cleared at t = 3.3 second by opening the faulted phase and reclosing it after 500 ms. The rapid injection of reactive current during fault recovery leads to a significant voltage overshoot reaching approximately 4.0 pu at the point of interconnection (POI), which causes the turbine to trip, as shown in Fig. 9. Note that each windfarm unit size is 3.5 MW.

However, if the event is detected as an SPT event and the turbine is configured to modify its reactive current injection behavior accordingly, it can successfully ride through the disturbance and continue delivering active power. This improved response is demonstrated in Fig. 10 and Fig. 11.

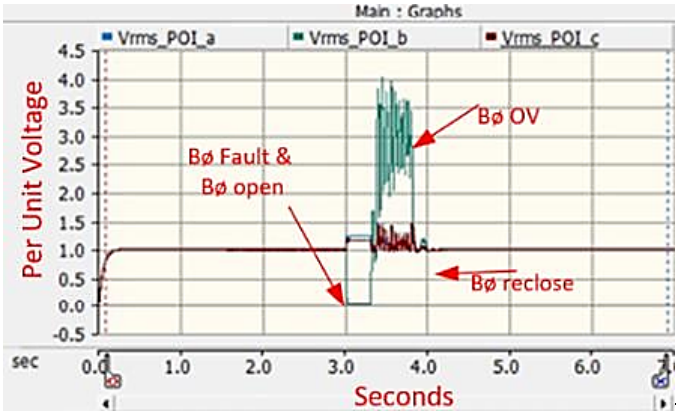

Fig. 8. POI Voltage Response to an 18-Cycle Fault Clearing and Reclosing on B-Phase

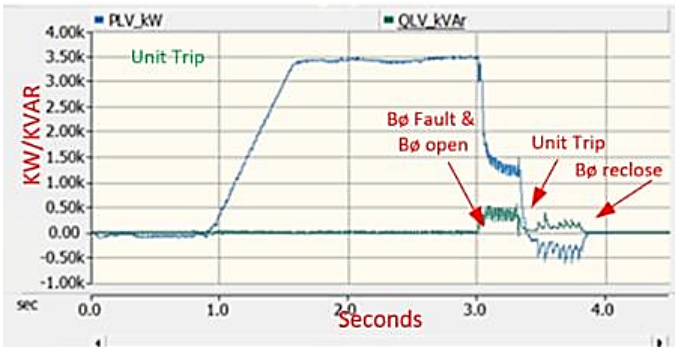

(a)

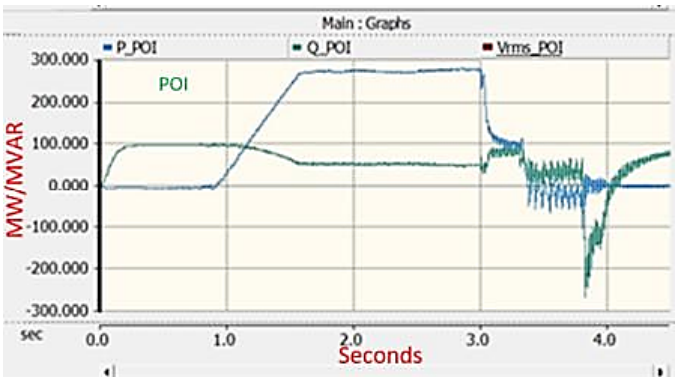

(b)

Fig. 9. Active and Reactive Power Response at the a) IBR Generator Terminal and b) POI to Fault Clearing and Reclosing on the B-Phase

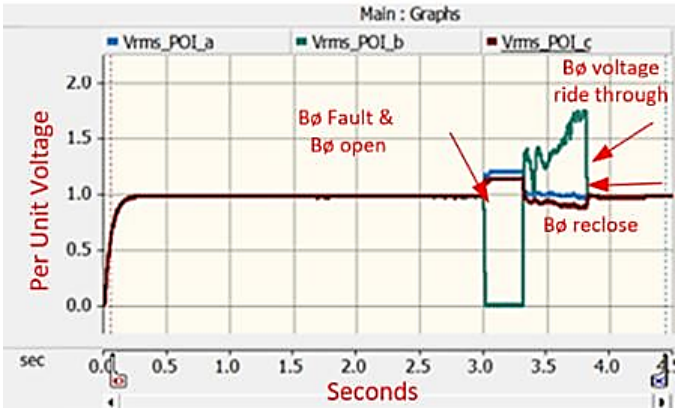

Fig. 10. POI Voltage Response to 18-Cycle Fault Clearing and Reclosing on the B-Phase After Modified Current Injection Algorithm

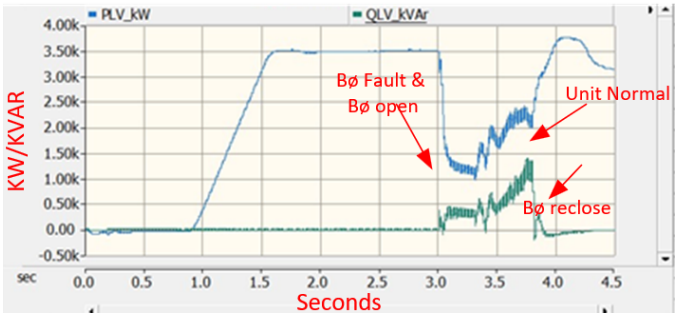

(a)

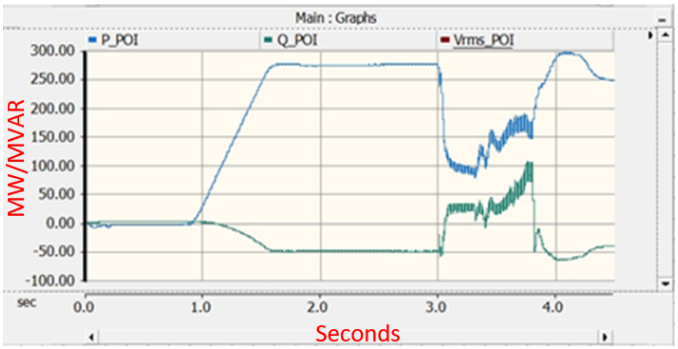

(b)

Fig. 11. Active and Reactive Power Response at the a) IBR Generator Terminal and b) POI to Fault Clearing and Reclosing on the B-Phase

V. SPT Events and Analysis

The following subsections summarize the key characteristics of four successful SPT field events, including reclosing in areas with high IBR penetration, related system observations, and the use of transient recording and neutral reactor monitoring to confirm successful reclosure. The subsections also provide a detailed analysis, supported by relay records and simplified one-line diagrams (not shown in Figure 1), which indicate breaker status (green for open, red for closed, and mark single-pole tripped breakers with red diagonal lines).

A. Summary of Successful SPT Field Events

1) Event 1: 345 kV W-P Line With Series Compensation and Shunt Reactors

Event 1 demonstrates successful fault clearing under high renewable penetration with midline series compensation and terminal shunt reactor support. The event confirms effective arc extinction and voltage recovery using standard SPT practices.

2) Event 2: 345 kV T-G Line With HVdc and Mixed IBR Terminals

Two single-phase faults on the same transmission line were successfully cleared using SPT, yet exhibited distinct transient behaviors due to differences in the NGR availability. In one case, the presence of the NGR supports stable system response during the open-pole interval. In the other case, the absence of the NGR leads to altered voltage redistribution and elevated fast-front overvoltage (FFOV) on the healthy phases. These transients are initiated by dielectric changes and capacitive coupling with limited damping from the IBR-only remote terminal. This event highlights the importance of selective NGR deployment, adaptive inverter control, and coordinated reactive support in maintaining system performance and insulation integrity in high IBR corridors. Waveform recordings with submillisecond resolution allow for detailed analysis of fault behavior and breaker operation, providing valuable insight into system dynamics during SPT events.

3) Event 3: 345 kV D-C Parallel Lines With VRT-Enabled IBRs

A single-phase fault along the D-C line corridor demonstrates consistent secondary arc behavior, stable voltages on healthy phases, and successful reclosing. VRT-enabled IBRs remained online, confirming the ride-through capability and coordinated system response.

4) Event 4: 345 kV T-B Line With Synchronous Condenser and Type 4 IBRs

Event 4 highlights the interaction between synchronous condensers and VRT-enabled IBRs during a B-phase-to-ground fault. The event reveals differences in arc suppression and recovery behavior between terminals, with successful reclosing and no IBR disconnection. The synchronous condenser at Station B played a key role in damping transients and supporting voltage recovery.

B. Details of Successful Field Events

1) Event 1: Single-Phase Fault on 345 kV W-P Line With Series Compensation and Shunt Reactors

Fig. 12 illustrates a simplified one-line diagram of the 118.60-mile, 345 kV W-P transmission line, which includes a midline series capacitor. The terminal at Station W is interconnected with three wind generation facilities: an 800 MW POI from a Type 3 wind plant directly connected at Station W, a 500 MW POI from a Type 4 wind facility, and a 1,005 MW POI from another Type 3 wind facility. These generation sources collectively supply power to the utility's network. Additionally, the terminal at Station P is interconnected with the utility's system. Both Station W and Station P are equipped with 72 MVAR shunt reactors, each grounded through neutral reactors.

Under a normal system configuration, SPT is applied for line-to-ground faults on this transmission line, while the series capacitor bank is configured to bypass only the faulted phase. However, for this event, all three capacitor phases are temporarily configured to bypass upon a single-phase fault detection, a deviation from standard SPT practice.

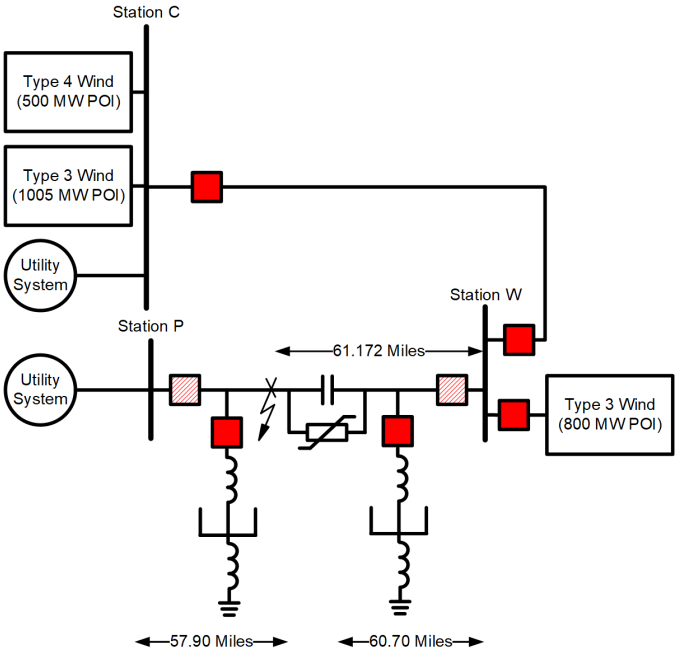

Fig. 12. Simplified One-Line Diagram of the 345 kV W-P Transmission Line

A B-phase-to-ground fault occurs approximately 61.2 miles from Station W on the 345 kV W-P transmission line. The fault initiates a voltage collapse consistent with arc formation. Relay records confirm timely initiation of SPT. During the open-pole interval, the B-phase voltage exhibits a damped oscillatory decay, indicative of a self-extinguishing secondary arc. No restrike is observed. Neutral reactor current measurements confirm arc conduction and suppression during the dead time, consistent with IEEE C37.109, *IEEE Guide for the Protection of Shunt Reactors* [10]. Fig. 13 and Fig. 14 display the relay records from Station W and Station P, respectively. Both of these figures show the phase currents, per-unit voltages of the healthy phases, instantaneous voltage of the faulted phase, and breaker status to illustrate the fault subsequent reclosure.

At Station W, the relay detects a faulted B-phase current surge reaching 3,400 A, as shown in Fig. 13, while the A- and C-phase voltages remain stable, showing minimal deviation from nominal levels. This behavior highlights the effectiveness of shunt reactor support and the interconnection stiffness at this terminal. At Station P, the B-phase fault current peaks at approximately 4,200 A, as shown in Fig. 14. Voltage magnitudes remain within expected limits with no anomalies observed. Breaker status records confirm proper pole opening and closing coordination at both terminals.

Immediately following the B-phase breaker opening, a transient deviation is observed in the A- and C-phase voltages. This short-duration fluctuation is attributed to the temporary three-phase bypassing of the midline series capacitor bank. Under normal conditions, the series capacitors contribute capacitive reactance that regulates voltage and reduces line impedance. Despite the fault being a single phase, the sudden removal of series capacitors across all phases introduces a momentary impedance unbalance, resulting in redistribution of the electric field and voltage stress across the healthy phases.

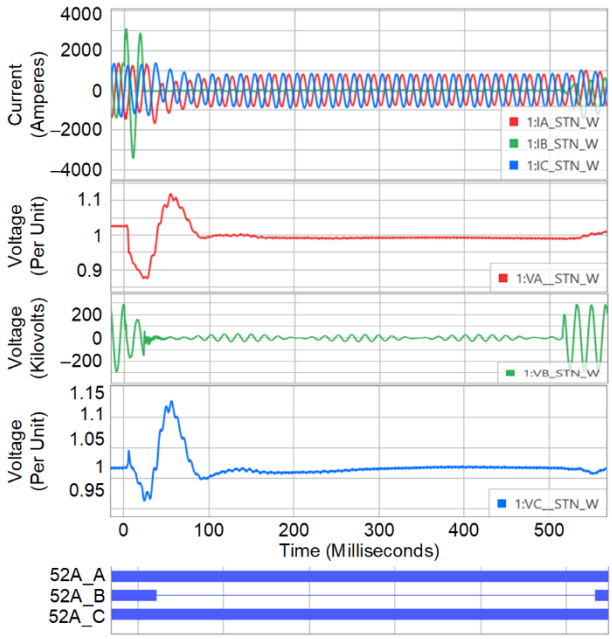

Fig. 13. Station W—Relay Record for BG Fault

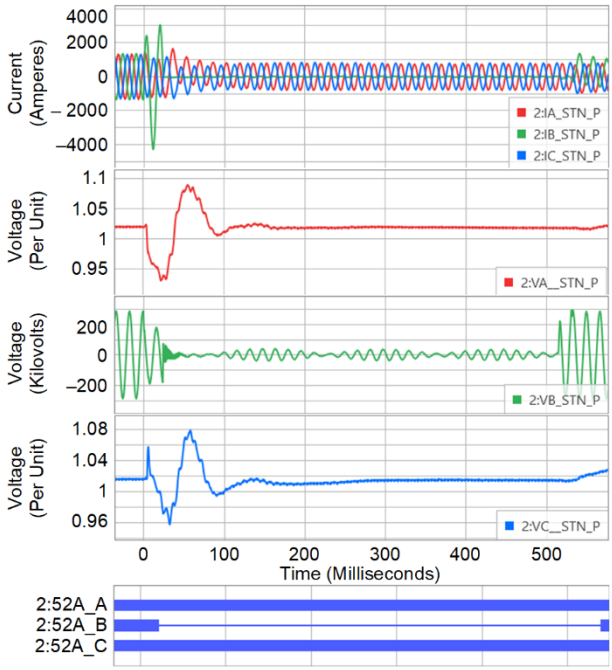

Fig. 14. Station P—Relay Record for BG Fault

This behavior aligns with known dynamics in series-compensated transmission systems, where bypassing capacitors can induce oscillatory excursions or voltage envelope distortions in nonfaulted phases due to interphase coupling and the abrupt change in reactive support. The presence of high-penetration IBRs further influences the system's transient response because the wind generation facilities momentarily react to the altered impedance and voltage profile. These deviations subside rapidly as the system rebalances and the fault-clearing sequence progresses.

The A-phase current modulation peaks at 1,600 A (see Fig. 13) and is primarily influenced by interphase capacitive coupling and the temporary three-phase bypassing of the

midline series capacitor during the fault event. This bypass alters the impedance balance of the transmission line, contributing to transient coupling effects and current distortion. Despite these conditions, system stability is maintained and protection coordination remains unaffected.

This event highlights the effective performance of SPT and protection coordination on the 345 kV W-P transmission line with high IBR integration. It also demonstrates the system's ability to maintain reliable operation and protection performance with modified line configurations, reinforcing the robustness of the protection scheme and the adaptability of the network.

2) Event 2: Single-Phase Faults on 345 kV T-G Line With NGR Variation

Fig. 15 presents a simplified one-line diagram of the 70.4-mile, 345 kV T-G transmission line and highlights the key elements at Station T and G.

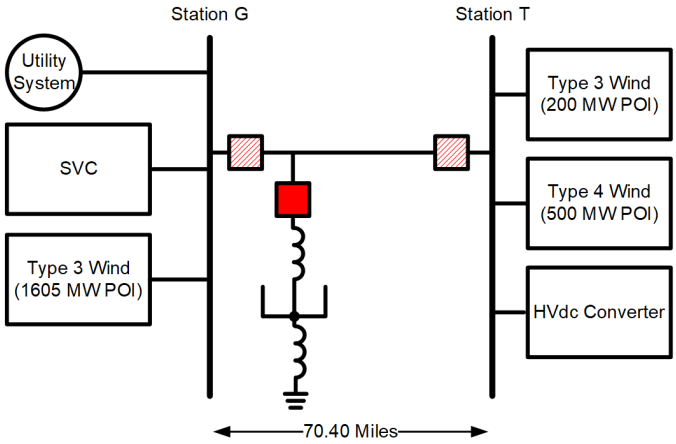

Fig. 15. Simplified One-Line Diagram of the 345 kV T-G Transmission Line

3) Case A: 345 kV T-G Line With NGR in Service

A C-phase-to-ground fault occurred approximately 31.65 miles from Station T on the 70.4-mile, 345 kV T-G transmission line. Fig. 16 and Fig. 17 display the relay records from Station T and Station G, respectively. These figures show the phase currents, pu voltages of the healthy phases, instantaneous voltage of the faulted phase, and breaker status to illustrate the fault clearing and subsequent reclosure.

Field-recorded waveforms, shown in Fig. 16, capture a peak C-phase fault current of 2,300 A at Station T. During the open-pole interval, the unfaulted A- and B-phase voltages increase to 1.190 pu and 1.247 pu, respectively. Even though the breaker pole was fully open at both terminals, the C-phase voltage is an expected open-phase response on a long, shunt-compensated EHV line. Capacitive coupling from the energized phases biases the floating conductor, while the NGR provides the inductive return. Together, they form a lightly damped, near-resonant zero-sequence network that sustains a quasi-steady potential rather than collapsing. This behavior is consistent with IEEE Std C37.109 [10] and does not indicate inadvertent energization.

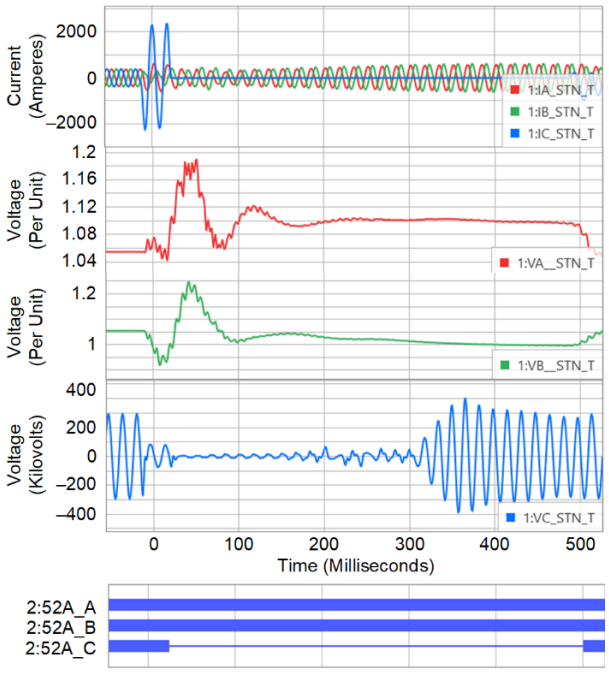

Fig. 16. Station T—Relay Record for CG Fault

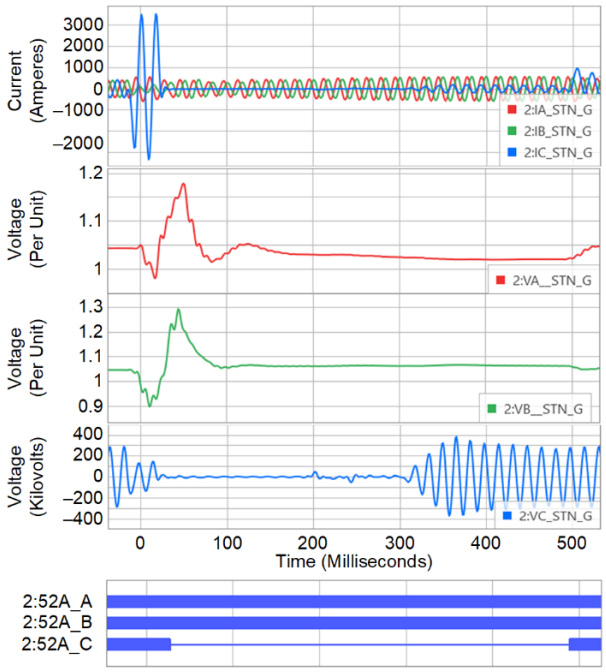

Fig. 17. Station G—Relay Record for CG Fault

All IBRs at Station T remain in service throughout the open-pole interval. The elevated voltages on the healthy phases remain within the VRT thresholds defined in IEEE Std 2800 [8]. No PLL instability or fault ride-through violations are observed. During the unbalanced fault, Type 4 IBRs sustain the induced C-phase potential by regulating positive-sequence voltage on the healthy phases without injecting significant negative-sequence current. This interaction occurs via interphase capacitive coupling and is further amplified by the lightly damped, near-resonant zero-sequence network formed by the floating conductor, coupling capacitance, and the NGR—a condition particularly pronounced on long, shunt-

compensated EHV lines. This characteristic phenomenon in high IBR penetration corridors is recognized in industry documents such as IEEE PES TR68, *Impact of Inverter Based Generation on Bulk Power System Dynamics and Short-Circuit Performance* [5]. In this event, Type 3 wind generation resources remain connected and provide dynamic voltage support consistent with their design characteristics. The HVdc station remains synchronized but passive, tracking system voltage without contributing fault current during the event.

At Station G, shown in Fig. 17, the fault current peaks at 3,407 A. This reflects a stronger grid connectivity and higher fault current availability. Voltage magnitudes on the unfaulted phases are more balanced, with A-phase reaching 1.179 pu and B-phase reaching 1.293 pu. These values remain within the acceptable limits for dynamic voltage support. The grounded 72 MVAR shunt reactor conducts measurable neutral current during arc extinction. The SVC at Station G further supports voltage regulation, mitigating overvoltage excursions during the open-pole interval.

This event demonstrates effective SPT and reclosing performance, even with one fully IBR-based terminal, provided that remote grounding and dynamic voltage support are present. The coordinated response of inverter controls, grounding infrastructure, and reactive support devices ensure stable fault clearance and dielectric recovery.

The utility performs event-based analysis to verify the integrity of neutral reactor connections. As outlined in IEEE C37.109 [10], neutral reactors are designed to remain nonconductive under normal operating conditions and only carry current during single-phase faults and breaker operations. The utility, along with other utilities, has observed failures in neutral reactor connections. To mitigate this risk, neutral reactor current is monitored during SPT events to confirm connection integrity.

The utility uses a 72 MVAR, 345 kV shunt reactor. The full-load current for this reactor can be calculated using (1).

$$I = \frac{Q}{\sqrt{3} \bullet V_{LL}} = \frac{72 \bullet 10^6}{\sqrt{3} \bullet 345 \bullet 10^3} \approx 120.5\ A \qquad (1)$$

where:

Q is the reactive power (72 MVAR).

V_{LL} is the line-to-line voltage (345 kV).

I is the full-load current.

During an SPT event on the T-G line (Event 2—Case A), the measured neutral reactor current peaks at 57.15 A (see Fig. 18). The expected current was calculated using the impedance-based formulation for zero-sequence current, which is shown in (2).

$$3I0 = \frac{V_{LN}}{X_L + 2X_{LN}} = \frac{\frac{345\ kv}{\sqrt{3}}}{1846 + 2 \bullet 1819} \approx 36\ A\ (rms) \qquad (2)$$

where:

X_L is the impedance of the shunt reactor (1846 Ω).

X_{LN} is the impedance of the neutral-ground reactor (1819 Ω).

V_{LN} is the line-to-neutral voltage $\left(\frac{V_{LL}}{\sqrt{3}}\right)$.

The observed peak current (36A rms $\bullet \sqrt{2} \approx$ 51 A peak) aligns with theoretical expectations, validating the connection integrity. A small amount of current is present before the fault due to current unbalance. A-phase and B-phase currents reach 161.41 A, shown in Fig. 18. This is consistent with the expected full-load range for the shunt reactor.

Shunt reactors, when interacting with line capacitance, can induce postdisturbance oscillations. These oscillations may occur near the system nominal frequency and influence the zero-sequence current measurements. The resonant frequency of the system is shown in (3).

$$f_R = f_S \bullet \sqrt{\frac{K_{sh}}{100}} \qquad (3)$$

where:

f_R is resonant frequency (Hz).

f_S is the system nominal frequency (60 Hz).

K_{sh} is the percentage of shunt compensation, shown in (4)

$$K_{sh} = \frac{\text{Total shunt reactor MVAR}}{\text{Line charging MVAR}} \times 100\% \qquad (4)$$

This formula estimates the frequency at which the inductive reactance of the shunt reactor and the capacitive reactance of the transmission line balance create a resonant condition. Such resonance can amplify post-fault oscillations and affect voltage recovery. For example, with $K_{sh} = 50\%$ shunt compensation, the resonant frequency would be (5).

$$f_R = \left(f_S \bullet \sqrt{0.5}\right) = 60 \bullet 0.7071 \approx 42.4\ Hz \qquad (5)$$

This calculation is based on IEEE Std C37.109 [10] guidance for shunt reactor applications.

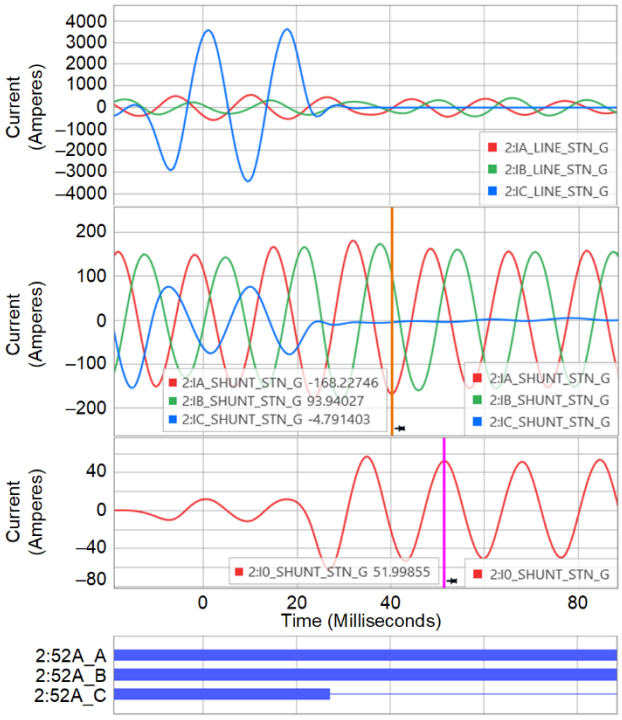

Fig. 18. Neutral Reactor Integrity Monitor

4) *Case B: 345 kV T-G Line With NGR Shorted and Out of Service*

A B-phase-to-ground fault occurred approximately 42.17 miles from Station G on the same 345 kV T-G transmission line. Unlike Case A, the NGR at Station G was temporarily shorted and out of service, which altered the post-fault clearing behavior. Fig. 19 displays the relay records from Station G and shows the pu phase currents at Station G and Station T, the sequence current from Station G, and the breaker status to illustrate the fault clearing and subsequent reclosure. Fig. 20 displays high-speed, submillisecond point-on-wave resolution of three-phase voltages, expressed as the voltage difference between Station G and an adjacent line terminal. Although the adjacent terminal is not shown in Fig. 15, its reference is included to indicate the differential voltage used to monitor breaker contact behavior. The waveform also includes instantaneous faulted-phase voltage and current, providing insight into fault inception and interruption dynamics. These data are captured using a UHS line relay equipped with advanced waveform recording capabilities. Such resolution enables observation of fast electrical transient and breaker contact behavior that are not typically captured using standard event reports. This differential measurement is used to monitor the voltage across breaker contacts indirectly and analyze transient recovery voltage-related stress during breaker contact operation. The plot also highlights FFOVs with sharp spikes on the healthy phases during fault interruption.

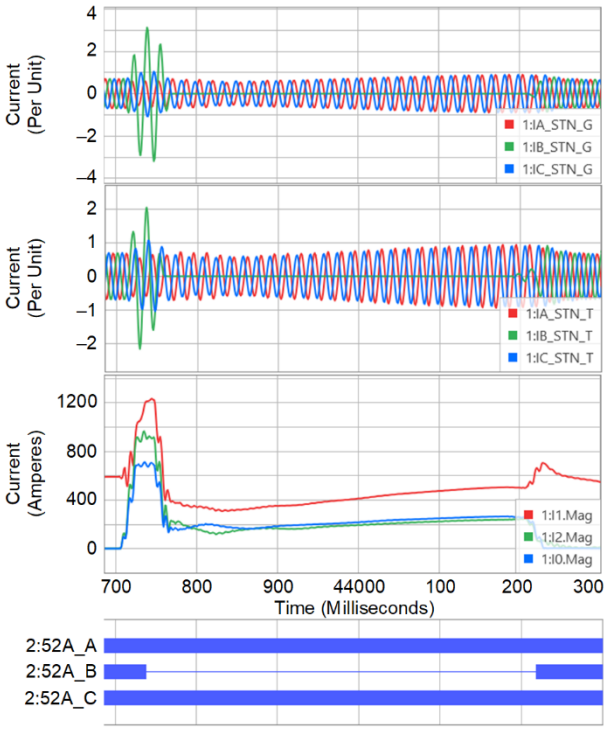

Fig. 19. Station G—Relay Record for BG Fault

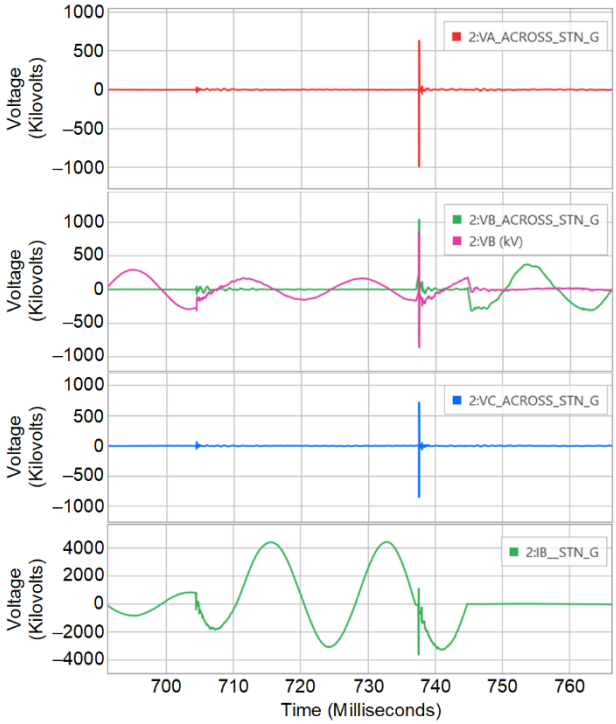

Fig. 20. Station G—Phase Voltage Differential With Adjacent Line and Faulted Phase Current

FFOVs are observed on the healthy A- and C-phases during the current interruption of the faulted B-phase (Fig. 20). These transients are initiated by rapid dielectric changes within the breaker with interphase capacitive coupling and zero-sequence voltage redistribution contributing to the rise in voltage on the unfaulted phases. The waveform characteristics, steep voltage gradients, and short front duration fall within the fast-front classification defined in IEEE Std C37.011, *IEEE Guide for the Application of Transient Recovery Voltage for AC High-Voltage Circuit Breakers with Rated Maximum Voltage above 1000 V* [11] and IEEE Std 2426, *IEEE Guide for Field Measurement of Fast-Front and Very Fast-Front Overvoltages in Electric Power Systems—Part 1: Measuring Techniques* [12]. Although specific waveform metrics for the healthy phase FFOVs are not presented here, the event exhibits high-frequency voltage excursions consistent with fast-front behavior. These conditions can impose significant voltage deviation on healthy phases even when their systems remain closed during faulted phase interruption.

The temporary bypass of the NGR at Station G eliminates a critical damping path for high-frequency components, enabling steep front surges to propagate along the unfaulted phases with minimal attenuation. With an IBR-only remote termination, the available negative-sequence support and high-frequency damping during the open-pole interval are limited, which further sustains the steep front content. This condition amplifies phase-to-ground voltages and transient energy levels. These observations underscore the importance of maintaining voltage stability on healthy phases and precise control of system contact behavior during fault interruption to mitigate FFOV exposure, particularly in systems with high line-to-line capacitive coupling and IBR terminals.

The fault events on the T-G transmission line underscore the influence of IBR behavior and NGR configuration on fault-clearing performance.

In Case A, the presence of the NGR at the strong terminal provides a zero-sequence return path that supports arc extinction and voltage stabilization. The IBR terminal remains synchronized, and voltages stay within IEEE Std 2800-2022 ride-through thresholds [8].

In Case B, the NGR is out of service, removing the zero-sequence path and altering voltage redistribution. FFOVs are observed on the healthy phases, initiated by dielectric changes and capacitive coupling. The IBR-only remote terminal lacks damping capability, allowing steep front transients to persist and increasing voltage deviation on healthy phases. These observations highlight the importance of selective NGR deployment, adaptive inverter control, and coordinated reactive support to ensure reliable fault clearance and voltage recovery in high IBR corridors, as emphasized in IEEE Std C37.04, *IEEE Standard for Ratings and Requirements for AC High-Voltage Circuit Breakers with Rated Maximum Voltage Above 1000 V* [13], IEC 62271-100:2021, *High-Voltage Switchgear and Controlgear*–Part 100: Alternating-Current Circuit-Breakers [14], and IEEE Std 2800 [8].

C. Event 3: Single-Phase Faults on 345 kV C-D Parallel Lines With VRT-Enabled IBRs

Fig. 21 presents a simplified one-line diagram of 345 kV C-D transmission corridor, which consists of two parallel lines connecting Station C to Station D.

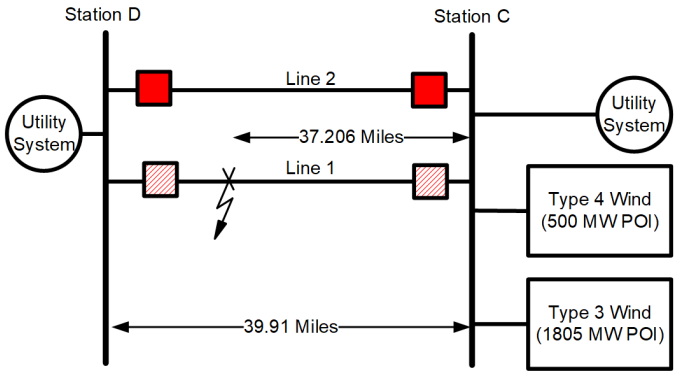

Fig. 21. Simplified One-Line Diagram of the Parallel 345 kV C-D Transmission Line

A C-phase-to-ground fault occurred approximately 37.2 miles from Station C on the 39.91-mile, 345 kV C–D transmission line. Fig. 22 and Fig. 23 display the relay records from Station C and Station D, respectively. These figures show the phase currents, pu voltages of the healthy phases, instantaneous voltage of the faulted phase, and breaker status to illustrate the fault clearing and subsequent reclosure.

At fault inception, the C-phase voltage collapse at both terminals. During the open-pole interval, healthy phase voltages at Station C reach minimum values of approximately 0.863 pu on the A-phase and 0.761 pu on the B-phase, shown in Fig. 22. These values, while below nominal, are compared against the continuous ride-through thresholds defined in IEEE Std 2800 [8], which specify a minimum of 0.90 pu for 3 seconds and 0.70 pu for 2.5 seconds. The voltage depression is attributed to a fault-induced current redistribution between the two parallel circuits, reactive power shift in the corridor, and transient IBR control response.

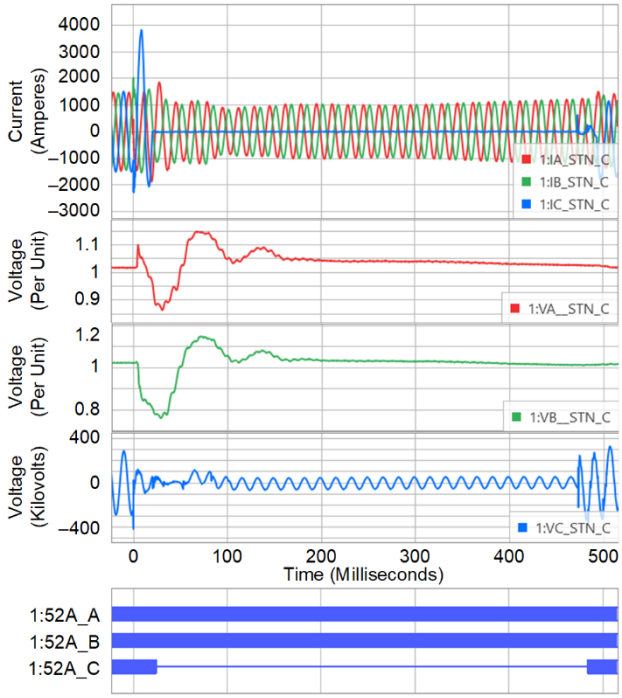

Fig. 22. Station C—Relay Record for CG Fault

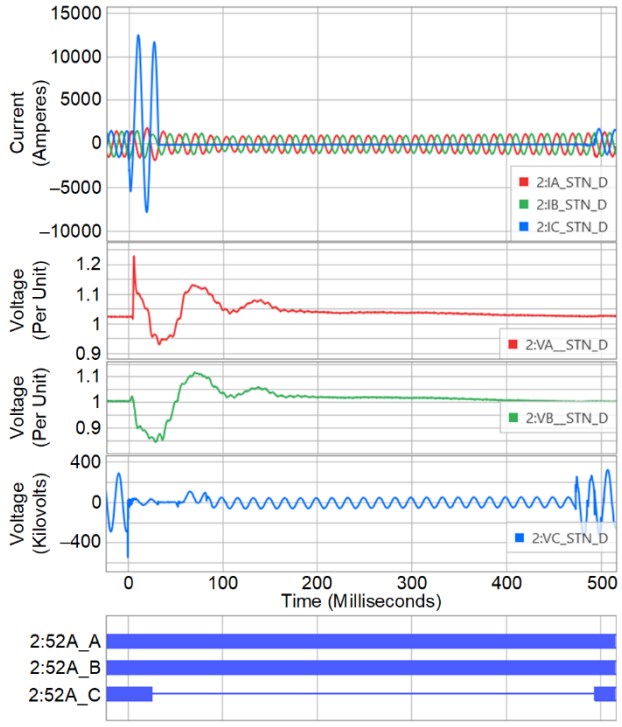

Fig. 23. Station D—Relay Record for CG Fault

Healthy phase voltage recovery during the dead time is supported by VRT-enabled IBRs at Station C, which maintains synchronism and reactive power injection throughout the interval. The strong source in the Station D terminal and the

parallel line path provide additional system stiffness, limiting the depth and duration of the voltage depression.

During the reclosing sequence, minor prestrike-related high-frequency transients are recorded at both terminals. These are short in duration and naturally damped by the network, with no indication of equipment stress or protection misoperation.

In summary, this event demonstrates that in a parallel line configuration, a single-line-to-ground fault can lead to brief healthy phase voltage dips caused by intercircuit current redistribution and reactive power unbalance. These transients are not operationally significant and do not result in protection misoperation. VRT-enabled IBRs at Station C maintain synchronism and reactive support, while the strong source Station D terminal and parallel line configuration provide system stiffness. This coordinated response ensures voltage recovery, secondary arc extinction, and compliance with IEEE Std 2800 ride-through requirements [8].

D. Event 4: Single-Phase Faults on 345 kV T-B Line With Mixed IBRs and Synchronous Condenser Support

Fig. 24 illustrates the simplified one-line diagram of the 345 kV T-B transmission corridor, which interconnects Station B and Station T. The wind plant at Station B is integrated through a three-winding 345/24 kV Yg/Yg/delta step-up transformer and a synchronous condenser at Station B provides dynamic voltage regulation and reactive power support.

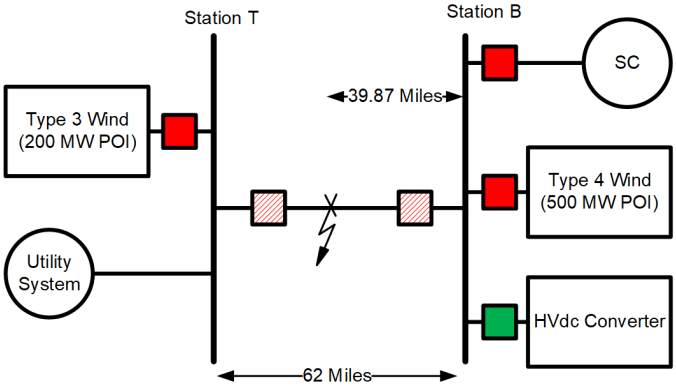

Fig. 24. Simplified One-Line Diagram of the 345 kV T-B Transmission Line

A B-phase-to-ground fault occurred approximately 39.85 miles from Station B on the 345 kV T-B transmission line. Fig. 25 and Fig. 26 display the relay records from Station T and Station B, respectively. These figures show the phase currents, pu voltages of the healthy phases, instantaneous voltage of the faulted phase, and breaker status to illustrate the fault clearing and subsequent reclosure.

At fault inception, Station T records a sharp increase in the B-phase current, accompanied by elevated negative- and zero-sequence components consistent with single-line-to-ground fault behavior. The B-phase voltage collapses as expected, while A- and C-phase voltages exhibit a brief rise but remain below the 1.2 pu threshold defined in IEEE Std 2800-2022 [8] for inverter VRT.

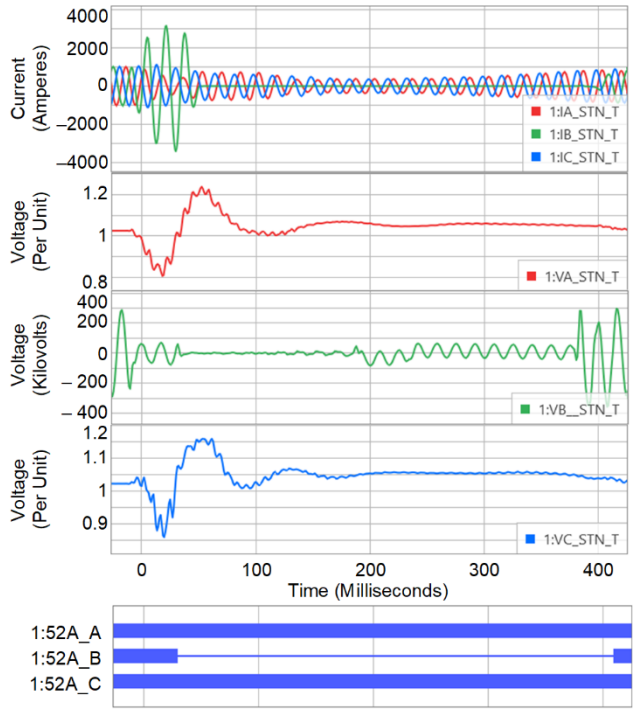

Fig. 25. Station T—Relay Record for BG Fault

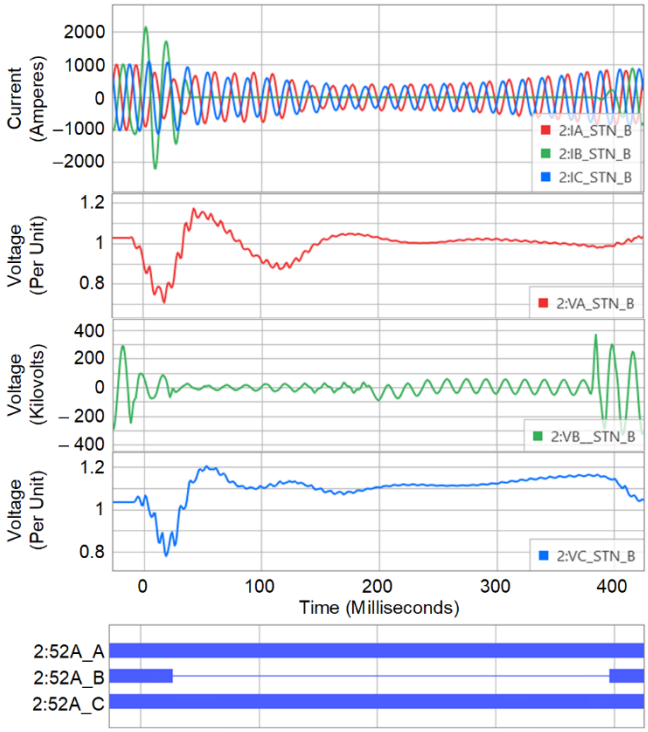

Fig. 26. Station B—Relay Record for BG Fault

Following the B-phase breaker opening at Station T, all phase voltages stabilize rapidly, with no restrike or significant postclearing oscillations. This response reflects prompt arc extinction and the stabilizing influence of the utility's system connection.

At Station B, initial fault waveforms are similar; however, the postclearing interval exhibits low-frequency oscillations in the B-phase voltage, indicative of secondary arc conduction sustained by capacitive coupling from the healthy phases and

residual trapped charge. These oscillations diminish naturally prior to reclosing and no restrike is observed, as confirmed by the disappearance of harmonics in the waveform. Healthy phase voltages remain within IEEE Std 2800 [8] limits throughout the open-pole interval, preventing IBR disconnection due to overvoltage logic.

The reclosing sequence at both terminals is free of significant prestrike or high-frequency transients. The synchronous condenser installed at Station B contributes to damping residual transients and supporting voltage recovery following breaker closure.

In summary, this event reinforces the effectiveness of the utility's SPT strategy in corridors with high IBR penetration. Successful SPT performance is achieved by maintaining healthy phase voltages within VRT thresholds and ensuring adequate reactive and damping support. Reactive support from the synchronous condenser at Station B, combined with system stiffness provided by the utility's grid connection at Station T, enables controlled arc extinction, stable voltage recovery, and reliable reclosing without IBR disconnection. Notably, the Type 4 IBRs at Station B remain online throughout the open-pole interval, demonstrating compliance with VRT criteria and confirming that well-tuned inverter controls can maintain stable operation under transient unbalanced voltage conditions. This case, alongside previous events, highlights the importance of adaptive protection, coordinated inverter behavior, and system-level support in maintaining grid resilience under high renewable integration.

VI. Conclusion

This paper reviews the PNM transmission system, the utility's standards and SPT protection schemes. The paper also discusses the response of IBR and traditional generation, various IBR challenges, and the importance of understanding the inverter responses. This paper subsequently discusses field-validated applications of SPT in a high IBR environment, highlighting both operational successes and protection challenges. Based on multiple 345 kV line corridor event analyses this paper proves that SPT is an effective solution for the utility to maintain system stability and reliability, even in regions dominated by high IBR (Type 3 and Type 4) wind and solar generation.

Sections III and IV of the paper discuss the limitations of traditional protection elements when applied near IBRs (i.e., reduced fault current levels, nondeterministic negative-sequence behavior and updates) required for protection philosophy [6] [15] [16] [17] [18]. The SPT events presented in Section V operated correctly under the utility's philosophy, including the use of zero-sequence directional elements near IBRs. Through careful system analysis and set point selection, misoperations in IBR system protection can be minimized or eliminated. This paper also emphasizes the need for updating the protection philosophy based upon IEEE standards, as well as incorporating insights from inverter manufacturers. A key takeaway is that multiple successful SPT field events near IBRs serve as valuable references and learning tools.

VII. Acknowledgments

The authors gratefully acknowledge the contributions of Venkat Mynam, Armando Guzmán, Fernando Calero, Jordan Bell, and Greg Smelich for their involvement in the validation of the lab test results, reviews, and discussions to improve settings for high IBR area and protection settings updates.

VIII. References

[1] H. Moradi, K. Garg, M. V. Mynam, E. Chua, and J. Bell, "PNM Approach to Protecting Overcompensated High-Voltage Lines," proceedings of the 72nd Annual Conference for Protective Relay Engineers, College Station, TX, March 2019.

[2] H. Moradi, D. Marquis, K. Garg, G. Smelich, and Y. Tong, "Testing and Commissioning Ultra-High-Speed Line Protection on a 345 kV Transmission Line," proceedings of the 72nd Annual Conference for Protective Relay Engineers, College Station, TX, March 2019.

[3] D. Marquis, M. Malichkar, A. Parikh, G. Smelich, and K. Garg, "Protecting EHV Transmission Lines Using Ultra-High-Speed Line Relays: A New Standard for PNM," proceedings of the 48th Annual Western Protective Relay Conference, Spokane, WA, October 2021.

[4] IEEE PES Technical Report PES-TR81, "Protection Challenges and Practices for Interconnecting Inverter Based Resources to Utility Transmission Systems," July 2020.

[5] IEEE PES Technical Report TR68, "Impact of Inverter Based Generation on Bulk Power System Dynamics and Short-Circuit Performance," July 2018.

[6] R. Chowdhury and N. Fischer, "Transmission Line Protection for Systems With Inverter-Based Resources – Part I: Problems," proceedings of the 74th Annual Conference for Protective Relay Engineers, virtual format, March 2021.

[7] A. Schöley and T. Jeinsch, "Small-Signal and Transient Stability Investigation of Inverter Grid Synchronization," proceedings of the 27th International Conference on Circuits, Systems, Communications, and Computers (CSCC), Rhodes (Rodos) Island, Greece, July 2023.

[8] IEEE Std 2800-2022, *IEEE Standard for Interconnection and Interoperability of Inverter-Based Resources (IBRs) Interconnecting with Associated Transmission Electric Power Systems*.

[9] R. McDaniel and Y. Shah, "Improving Ground Fault Sensitivity for Transmission Lines Near Inverter-Based Resources," proceedings of the 50th Annual Western Protective Relay Conference, Spokane, WA, October 2023.

[10] IEEE Std C37.109-2023, *IEEE Guide for the Protection of Shunt Reactors*.

[11] IEEE Std C37.011-2019, *IEEE Guide for the Application of Transient Recovery Voltage for AC High-Voltage Circuit Breakers with Rated Maximum Voltage above 1000 V*.

[12] IEEE Std 2426-2024, "*IEEE Guide for Field Measurement of Fast-Front and Very Fast-Front Overvoltages in Electric Power Systems—Part 1: Measuring Techniques*."

[13] IEEE Std C37.04-2018, *IEEE Standard for Ratings and Requirements for AC High-Voltage Circuit Breakers with Rated Maximum Voltage Above 1000 V*.

[14] IEC 62271-100, *High-Voltage Switchgear and Controlgear*–Part 100: Alternating-Current Circuit-Breakers, 2021.

[15] E. Godoy, A. Celaya, H. J. Altuve, N. Fischer, and A. Guzmán, "Tutorial on Single-Pole Tripping and Reclosing," proceedings of the 39th Annual Western Protective Relay Conference, Spokane WA, October 2012.

[16] J. Esztergalyos, J. Andrichak, D. H. Colwel1, D. C. Dawson, J. A. Jodice, T. J. Murray, K. K. Mustaphi, G. R. Nai1, A. Politis, J. W. Pope, G. D. Rockefeller, G. P. Stranne, D. Tziouvaras, and E. O. Schweitzer, Single Phase Tripping and Auto Reclosing of Transmission Lines: IEEE Committee Report, IEEE Transactions on Power Delivery, Vol. 7, Issue 1, January 1992.

[17] F. Calero and D. Hou, "Practical Considerations for Single-Pole-Trip Line-Protection Schemes," proceedings of the 31st Annual Western Protective Relay Conference, October 2004.

[18] B. Kasztenny, "Distance Elements for Line Protection Applications Near Unconventional Sources," proceedings of the 75th Annual Conference for Protective Relay Engineers, College Station, TX, March 2022.

IX. Biographies

Daniel Marquis is a protection engineer at Public Service Company of New Mexico (PNM). Prior to working at PNM, he worked for the consulting firm TRC and attended graduate school at New Mexico State University (MSEE, 2009). He completed his undergraduate degree at Iowa State University (BSEE 2004). His research interests include alternative energy in remote areas and microgrids.

Errol Singer received his Bachelor of Science in Electrical Engineering from The University of New Mexico. He has over 30 years of utility experience with Public Service Company of New Mexico (PNM). Errol began his career as a distribution engineer, responsible for overhead and underground design. He later transitioned into the protection field, where he spent eight years in distribution protection and currently serves as a transmission protection engineer.

Melvin Bowekaty received his Bachelor of Science in Electrical Engineering from The University of New Mexico in 2008. He joined Public Service Company of New Mexico (PNM) in 2014 as a transmission protection engineer. Melvin is a registered professional engineer in the state of New Mexico.

Chelsea Collette received her BSECE degree from Oregon State University (OSU). Chelsea worked at Pacific Gas and Electric Company (PG&E) for about five years in various roles and spent the final two years in Protection Engineering. In 2020, Chelsea moved to Public Service Company of New Mexico (PNM) and has been working in protection engineering. Chelsea served as a protection engineer until 2023, when she moved to the role of team manager.

Samir Dahal holds a PhD in electrical engineering from the University of North Dakota and works as a senior key expert at Siemens Gamesa. He supports wind power projects throughout their full lifecycle, ensuring compatibility with evolving utility and regulatory requirements. His expertise spans technical modeling, compliance, and grid integration, contributing to the reliable deployment of sustainable energy systems across North America.

Ashish Parikh received his BEEE from Nirma Institute of Technology, Gujarat University, Ahmedabad, Gujarat, India. Ashish began his career at Schweitzer Engineering Laboratories, Inc. (SEL) as a field application engineer in the India branch office. He rose to the rank of senior application engineer before transferring to SEL Engineering Services, Inc. (SEL ES) in Pullman, Washington, where he is currently an engineer in the protection group. Ashish maintains a high level of technical expertise in electric power system protection, system fault analysis, commissioning, and technical training. He also possesses a working level of technical expertise in electric power system automation. He routinely performs power system modeling for short-circuit, load flow, and arc-flash studies, as well as protective device coordination. In addition, he is involved with event report analysis, protection scheme design, relay settings and coordination, and relay selection.

Milind Malichkar received his MSEE from Michigan Technological University in 2012 and his BSEE from Sardar Patel College of Engineering, Mumbai University, India, in 2005. Milind worked for Voltas Limited (IOBG), India, and Electromechanical & Technical Associates (ETA), Abu Dhabi, UAE, as a project engineer for five years before joining Schweitzer Engineering Laboratories, Inc. (SEL) in 2012. Currently, he is working as a project engineer supervisor at SEL Engineering Services, Inc. (SEL ES). Milind has experience in power system protection design and commissioning, short-circuit and coordination studies, and power system modeling and testing using control and power hardware-in-the-loop testing with a real-time digital simulator. He is a licensed professional engineer in the states of Washington, California, Alaska, and Arizona.

Kamal Garg received his MSEE from Florida International University and Indian Institute of Technology, Roorkee, India, and his BSEE from Kamla Nehru Institute of Technology, Avadh University, India. Kamal worked for Power Grid Corporation of India Limited and Black & Veatch for several years at various positions before joining Schweitzer Engineering Laboratories, Inc. (SEL) in 2006. Currently, he is a principal engineer at SEL Engineering Services, Inc. (SEL ES). Kamal has experience in protection system design, system planning, substation design, operation, remedial action schemes, synchrophasors, testing, and maintenance. Kamal is a licensed professional engineer in the United States and Canada, a senior member of IEEE, a chair and member of many working groups in the IEEE Power System Relaying and Control Committee (PSRC), and vice chair of PSRC K-Substation Protection Subcommittee. Kamal leads the IEEE Power & Energy Society (PES) Workforce Initiative (2023–2025) and holds four patents.